

Published in final edited form as:

Nat Cell Biol. 2016 February ; 18(2): 225–233. doi:10.1038/ncb3296.

De novo DNA methylation drives 5hmC accumulation in mouse zygotes

Rachel Amouroux¹, Buhe Nashun^{#1}, Kenjiro Shirane^{#2}, Shoma Nakagawa^{#3}, Peter WS Hill¹, Zelfa D'Souza¹, Manabu Nakayama⁴, Masashi Matsuda⁵, Aleksandra Turp¹, Elodie Ndjetehe¹, Vesela Encheva^{1,6}, Nobuaki R Kudo³, Haruhiko Koseki⁵, Hiroyuki Sasaki², and Petra Hajkova^{1,*}

¹Medical Research Council Clinical Sciences Centre, Imperial College London, London W12 0NN, United Kingdom.

²Division of Epigenomics and Development, Medical Institute of Bioregulation, Kyushu University, 3-1-1 Maidashi, Higashi-ku, Fukuoka 812-8582, Japan.

³Institute of Reproductive and Developmental Biology, Imperial College London, London W12 0NN, United Kingdom.

⁴Chromosome Engineering Team, Department of Technology Development, Kazusa DNA Research Institute, 2-6-7 Kazusa-Kamatari, Kisarazu, Japan.

⁵Laboratory for Developmental Genetics, RIKEN Center for Integrative Medical Sciences, 1-7-22 Suehiro, Tsurumi-ku, Yokohama, Japan.

These authors contributed equally to this work.

Abstract

Zygotic epigenetic reprogramming entails genome-wide DNA demethylation that is accompanied by *Ten-Eleven Translocation 3* (Tet3)-driven oxidation of 5-methylcytosine (5mC) to 5-hydroxymethylcytosine (5hmC)¹⁻⁴. Here we demonstrate using detailed immunofluorescence analysis and ultra-sensitive LC/MS based quantitative measurements that the initial loss of paternal 5mC does not require 5hmC formation. Small molecule inhibition of Tet3 activity as well as genetic ablation impedes 5hmC accumulation in zygotes without affecting the early loss of paternal 5mC. Instead, 5hmC accumulation is dependent on the activity of zygotic Dnmt3a and Dnmt1, documenting a role for Tet3 driven hydroxylation in targeting *de novo* methylation activities present in the early embryo. Our data thus provide further insights into the dynamics of

Users may view, print, copy, and download text and data-mine the content in such documents, for the purposes of academic research, subject always to the full Conditions of use:http://www.nature.com/authors/editorial_policies/license.html#terms

*Correspondence should be addressed to PA: petra.hajkova@csc.mrc.ac.uk.

⁶present address: Cancer Research UK, Clare Hall Laboratories, South Mimms EN6 3LD, United Kingdom.

AUTHORS CONTRIBUTIONS

P.H. and R.A. conceived the study and wrote the manuscript with the assistance from H.S. and N.K. R.A. performed the experiments with the help of Z.S., P.W.H; R.A. and P.H. analysed the data. B.N. carried out micromanipulation of zygotes, and provided technical assistance. S.N. performed SCNT with the assistance of B.N. and R.A. R.A. and A.T performed the LC/MS experiment and analysed the data with the help of V.E. H.S provided the Dnmt1, Dnmt3a and Dnmt3L knockout mice and K.S. performed the IVF experiments. E.N. carried out Tet3 targeting in ES cells and generated Tet3 chimera. M.N, M.M. and H.K. provided the Tet3 KO mice.

COMPETING FINANCIAL INTERESTS

The authors declare no competing financial interests.

zygotic reprogramming revealing intricate interplay between DNA demethylation, *de novo* methylation and Tet3 driven hydroxylation.

In the mouse zygote, the paternal genome undergoes genome-wide loss of DNA methylation shortly after fertilisation^{5, 6}. This has been mainly attributed to the activity of the Tet3 hydroxylase responsible for the accumulation of 5hmC on the paternal DNA^{1, 3, 4}. To elucidate the exact involvement of 5hmC during this DNA demethylation, we examined the detailed kinetics of 5hmC appearance in connection with loss of 5mC signal (Fig. 1a,b). We confirmed accumulation of 5hmC in the paternal pronucleus at late zygotic stages¹⁻⁴, consistent with the described localisation and expression pattern of the Tet3 enzyme (Supplementary Fig. 1a,b). Detailed analysis of 5mC and 5hmC immunofluorescence data, however, revealed that while 5mC disappears from the paternal genome by early PN3 stage, 5hmC starts to accumulate only after the major drop in 5mC has occurred, and increases considerably from PN4 onwards (Fig. 1a-c)⁷. Consequently, paternal DNA of late PN2-early PN3 zygotes shows neither 5mC nor 5hmC signal (Fig. 1d). Moreover, the accumulation of 5-formylcytosine (5fC) and 5-carboxylcytosine (5caC)⁸⁻¹⁰ is detectable concomitantly to 5hmC appearance in paternal pronucleus, a few hours after the loss of 5mC (Supplementary Fig. 1c)¹⁰. The delayed appearance of 5hmC is also not due to the low sensitivity of the 5hmC antibody, as 5hmC is detectable with considerably higher sensitivity than 5mC (Supplementary Fig. 1d,e).

Tet proteins belong to the family of 2-oxoglutarate (2OG) and iron (Fe²⁺)-dependent dioxygenases¹¹. In order to assess the involvement of Tet3 driven 5mC hydroxylation in zygotic demethylation, we eliminated 5hmC by using dimethylallyl glycine (DMOG), a small molecule inhibitor of 2OG-dependent oxygenases. DMOG effectively blocks the activity of Tet enzymes *in vitro* (Supplementary Fig. 2a); consequently, the presence of DMOG during *in vitro* fertilisation (IVF) leads to an absence of 5hmC, 5fC and 5caC in the paternal pronucleus (Fig. 2a and Supplementary Fig. 2c,d). Of note, DMOG treatment does not affect the presence of maternal 5hmC (Fig. 2a), the normal asymmetry of histone modifications observed between pronuclei (Supplementary Fig. 3a), or the development of pre-implantation embryos (Supplementary Fig. 2e,f). Strikingly, the lack of 5hmC formation upon DMOG treatment did not impact on the extent of DNA demethylation in early mouse zygotes (PN3) (Fig. 2a and Supplementary Fig. 2b), which reinforced our initial observations showing that loss of paternal 5mC signal and accumulation of 5hmC are temporally disconnected. We further confirmed our findings by inhibiting Tet3 activity in the zygote using a Fe²⁺ chelator, deferoxamin (DFX). This inhibitor also effectively blocks the formation of 5hmC, but has no impact on the loss of paternal 5mC signal in the early PN3 zygotes (Supplementary Fig. 3b,c), as also observed with DMOG. Collectively, these results suggest that the Tet3-driven accumulation of 5hmC observed in the late zygote is not required for the initial loss of paternal 5mC signal.

Line1 represents a class of non-LTR repetitive elements that has been shown to lose methylation during zygotic reprogramming^{5, 12, 13}. Although these elements have been previously suggested as targets for 5mC hydroxylation in zygotes^{2, 3}, our results clearly show that *Line1* elements (L1Md_Tf and L1Md_Gf subtypes) undergo DNA demethylation

in the absence of 5hmC formation to a similar extent as that observed in the control zygotes and 2-cell stage embryos (Supplementary Fig. 3d,e).

Immunofluorescence analysis provides an indirect quantification of DNA modifications, relying on the specificity and the affinity of the antibodies used. Additionally, differences between staining protocols, signal acquisition and approaches used to normalise the resulting signal make direct comparison between studies problematic. Bisulphite analysis can provide sequence specific information, however the results are compromised by the inability to distinguish between 5mC and 5hmC and between C, 5fC and 5caC^{8, 9, 14}. In addition, whole genome bisulphite analysis is subject to amplification biases and the lack of information regarding the copy number of various repetitive elements in the genome precludes precise quantitative assessment of the dynamic changes in global DNA modifications. Considering these facts we further supported our findings by independent quantitative approach using an ultra-sensitive LC/MS method (Supplementary Fig. 4a).

Quantitative assessment of 5mC levels in normal fertilised zygotes (PN4-5) by LC/MS showed a clear 5mC loss in comparison with 5mC values measured in either of the gametes (Fig. 2b, Supplementary Fig. 4e) providing an additional evidence for zygotic DNA demethylation. To assess the relative contribution of parental genomes to the measured 5mC levels, we quantified 5mC in parthenogenetically activated oocytes that lack the contribution of sperm derived genome. Our LC/MS measurements show that parthenotes contain quantitatively similar amount of 5mC as MII oocytes ($p=0.075$, t -test) (Supplementary Fig. 4c). The global level of DNA methylation is also not significantly affected by DNA replication as shown by 5mC levels in parthenotes treated with aphidicolin ($p=0.078$, t -test) (Supplementary Fig. 4b,c). As the maternal methylation remains globally stable (Supplementary Fig. 4c), the measured 5mC quantity in zygotes implies that paternal genome at PN4-5 (10hrs post-fertilisation) has lost ~70% of 5mC compared to the sperm (Supplementary Fig. 4d). We confirmed that this measured loss of global 5mC occurs independently of the completion of S-phase ($p=0.058$ between control and aphidicolin-treated zygotes, t -test) (Supplementary Fig. 4f-h). Although we cannot preclude that demethylation of some loci requires S-phase progression^{15, 16}, our quantitative measurements demonstrate that on a genome-wide level the zygotic DNA demethylation is predominantly an active, replication-independent process (Supplementary Fig. 4f-h)^{5, 17, 18}.

Our LC/MS data further shows that the absolute 5hmC level in zygotes is very low compared to the amount of paternal 5mC lost during this wave of DNA demethylation (Fig. 2b and Supplementary Fig. 4e). Importantly and confirming our immunofluorescence data (Fig. 2a and Supplementary Fig. 2b), the measured global loss of 5mC is not affected by the absence of 5hmC in the DMOG-treated zygotes. These results thus demonstrate that 5hmC is not required for removal of the majority of 5mC in the early PN3 zygotes (Fig. 2a,b and Supplementary Fig. 4e).

To provide further genetic validation of our results, we generated a conditional oocyte specific *Tet3* knockout mouse model (Figure 3a). *Gdf9-Cre* driven *Tet3* deletion in early oocytes resulted in a complete absence of *Tet3* mRNA in *Tet3*^{mat-} MII oocytes ($p<0.001$, t -test, Fig. 3b) and *Tet3* protein in zygotes (Fig. 3c). This results in a lack of 5hmC formation

in the paternal pronucleus following fertilisation as assessed by immunofluorescence and by LC/MS of zygotes (Fig. 3d,e)³. In agreement with our data using dioxygenase inhibitors (Fig. 2a,b, Supplementary Fig. 3c), ablation of maternal Tet3 did not affect early loss of paternal 5mC observed in PN3 zygotes by immunofluorescence (Fig. 3d and Supplementary Fig. 4i) nor global 5mC levels in Tet3^{mat-/pat+} zygotes as measured by LC/MS (Fig. 3e). Combined, these results thus do not corroborate the currently accepted model whereby 5hmC is an intermediate for global DNA demethylation that occurs in early pre-replicative (PN3) mouse zygotes¹⁻⁴.

Further assessment of DMOG-treated and Tet3^{mat-/pat+} zygotes revealed that while the initial DNA demethylation proceeded normally in the absence of 5hmC formation, a slight accumulation of 5mC was detectable by immunofluorescence in the paternal pronucleus of later (late PN4-PN5) stage zygotes (Fig. 2a, 3d and Supplementary Fig. 2b, 4i). Although our LC/MS measurements did not detect any significant difference in 5mC in either Tet3^{mat-/pat+} or DMOG-treated zygotes, likely due to pooling of slightly different stages of zygotes (Fig. 2b, 3e and Supplementary Fig. 4e), loss of 5hmC in the zygote leads to a detectable, albeit small, increase in 5mC in the 2-cell stage embryos derived from DMOG-treated (Fig. 2c, $p < 0.001$, *t*-test) and Tet3^{mat-/pat+} zygotes (Fig. 3f, $p < 0.05$, *t*-test). The observed limited accumulation of 5mC in late stage Tet3 knockout and DMOG-treated zygotes is in agreement with the previously described contribution of Tet3 to zygotic DNA demethylation^{1, 3, 4}. However, and contrary to previous interpretation, our data document that the accumulation of 5mC occurs only once the initial wave of DNA demethylation has been completed (Fig. 1c, 2a, 3d and Supplementary Fig. 2b, 4i).

The accumulation of 5mC in paternal pronucleus of late stage DMOG-treated or Tet3-depleted zygotes indicates the presence of *de novo* methylation activity. However, the current models of zygotic epigenetic reprogramming assume the lack of 5mC maintenance during replication in the mouse preimplantation embryos^{13, 19}. Additionally, given the general loss of DNA methylation during zygotic and early preimplantation development^{5, 6, 13, 17}, the role or even existence of *de novo* DNA methylation in the early embryos has not been previously considered. To revise this assumption, we investigated the presence of maintenance and *de novo* DNA methylation activities in the zygotes using isotope labelling. The addition of isotope-labelled methionine during the IVF procedure resulted in a clear incorporation of labelled 5mC (5mC*) detectable in late-stage (PN4-5) zygotes (Fig. 4a). This signal is reduced, but still clearly detectable, following treatment with aphidicolin (Fig. 4a) unambiguously demonstrating that both the maintenance (replication coupled) and *de novo* (replication independent) methylation activities are present in the mouse zygote.

This prompted us to consider whether the late appearance of 5hmC in paternal pronuclei could be mechanistically linked to the zygotic DNA methylation activity rather than to the sperm derived 5mC as proposed in the current models^{1, 3, 4}. We carried out IVF in the presence of 5-azadeoxycytidine (azadC), an inhibitor of DNA methyltransferases that requires incorporation into DNA during replication. Zygotes incubated with azadC show a significant decrease in 5hmC level in the paternal pronucleus (Fig. 4b), demonstrating that 5hmC accumulation is linked to the generation of new zygotic 5mC. Notably, no significant

difference in paternal 5mC is observed in azadC-treated zygotes, either by immunofluorescence or by bisulphite sequencing of *Line1* elements (Supplementary Fig. 4j). This suggests that following the zygotic S-phase the observed *de novo* DNA methylation is limited and the majority of newly deposited 5mC is converted to 5hmC on the paternal genome. This conclusion is in agreement with the low absolute levels of 5hmC measured by LC/MS (Fig. 2b).

Previous reports have demonstrated the role of Dnmt3a and Dnmt3L in *de novo* DNA methylation during oocyte growth²⁰⁻²⁴. In early mouse zygotes both Dnmt3a and Dnmt3L show pronuclear localisation with progressive enrichment until PN5 (Supplementary Fig. 5a)^{25, 26}. To address whether Dnmt3a/3L driven *de novo* DNA methylation could provide a template for 5hmC formation during zygotic development, we assessed 5hmC levels in zygotes maternally depleted for Dnmt3a (Dnmt3a^{2lox/2lox}, Zp3-Cre) and Dnmt3L (Dnmt3L^{-/-}). Consistent with previous reports, the lack of maternally inherited Dnmt3a and Dnmt3L results in loss of DNA methylation in the maternal genome (Fig. 4c and Supplementary Fig. 5b)^{20, 24, 27, 28}. Additionally, the loss of maternal Dnmt3a, but not Dnmt3L (Fig. 4c and Supplementary Fig. 5b), leads to significantly reduced paternal 5hmC in PN4 zygotes. We thus conclude that Dnmt3a driven *de novo* DNA methylation is required for 5hmC formation in late zygotes.

Paternal accumulation of 5hmC is severely affected but not completely abolished in zygotes lacking Dnmt3a indicating a potential activity of another DNA methyltransferase. As Dnmt1 has been previously demonstrated to be present in both fully grown oocytes^{20, 29} as well as in early mouse embryos^{26, 30, 31}, we have assessed the potential contribution of maternal Dnmt1 for the accumulation of 5hmC using the oocyte specific Dnmt1 knockout [Dnmt1^{2lox/2lox}, Zp3-Cre]³². Interestingly, the lack of maternal Dnmt1 also leads to significantly lower levels of paternal 5hmC following fertilisation (Fig. 4d). The reduced paternal 5hmC in Dnmt3a and Dnmt1 KO zygotes is observed despite of the normal presence and localisation of Tet3 protein in these zygotes (Fig. 4e,f). Cumulatively our results demonstrate that in the zygote, both Dnmt3a and Dnmt1 generate new 5mC that is targeted for hydroxylation.

To further validate the presence of *de novo* activity in the ooplasm and the role of 5hmC in targeting newly deposited 5mC, we performed somatic cell nuclear transfer (SCNT) using wild type (WT) and triple knockout Dnmt3a^{-/-}, Dnmt3b^{-/-}, Dnmt1^{-/-} (TKO) ESCs³³ as donor cells (Fig. 5a). As expected, the nuclei of TKO ESCs are devoid of both 5mC and 5hmC (Supplementary Fig. 5c). 5hrs post-activation, 5mC and 5hmC are detected in WT-ESC pseudopronucleus whereas the fully decondensed TKO-ESC pseudopronucleus does not show appreciable amount of DNA modifications (Fig. 5a). However, 14hrs post-activation both the WT-ESC and the TKO-ESC pseudopronuclei display comparable levels of 5mC and 5hmC (Fig. 5a). The presence of both DNA modifications on the originally 5mC/5hmC-free DNA template further demonstrates the presence of previously unappreciated *de novo* DNA methylation activities in the ooplasm and that Tet3 targets the newly formed 5mC. Interestingly, pericentromeric heterochromatin in WT-ESC and TKO-ESC derived pseudopronucleus is enriched for 5mC but not for 5hmC (Supplementary Fig.

5d) replicating the pattern observed on the paternal genome in PN4 zygote (Supplementary Fig. 5e)³⁴.

Our detailed investigation of DNA modification dynamics in the zygote has revealed that 5hmC accumulation follows, but is not concomitant with, the loss of 5mC in the early (PN2-3) paternal pronucleus (Fig. 1). Furthermore, we have shown that the initial loss of paternal 5mC can be mechanistically uncoupled from 5hmC formation using a genetic loss of function model and small molecule inhibitors of dioxygenases, providing mechanistic proof that these processes are independent (Fig. 2, 3 and Supplementary Fig. 2b-d, 3c, 4d,e,i). In this context it should be noted that the methylation analysis of embryos depleted for Tet3 has been previously conducted on late stage (PN5) zygotes, which has left the dynamics of the DNA demethylation process under-appreciated^{1, 3, 7}.

The exact mechanism by which DNA demethylation proceeds in the zygote remains subject of an intense scientific debate, with both active and passive models proposed^{1-4, 15, 16, 35-37}. Our study shows that, quantitatively, the majority of observed global DNA demethylation proceeds independently of replication (Supplementary Fig. 4c,g,h) confirming previous bisulphite sequencing data^{5, 6, 13, 35}. Although we cannot rule out that a small proportion of loci lose their methylation through dilution^{15, 16}, this pathway provides only a limited contribution to the global methylation changes in the zygote. Combined with our findings regarding lack of major role of Tet3 driven oxidation, our data advocate the existence of an alternative mechanism implicated in the loss of paternal 5mC in the early (PN2-PN3) zygotes. In this context we note that both control and DMOG-treated zygotes show normal enrichment of chromatin bound XRCC1 DNA repair protein in the paternal pronucleus (Supplementary Fig. 5f), suggesting that the previously reported activation of the Base Excision Repair (BER) pathway^{7, 18} during DNA demethylation in the mouse zygotes does not require Tet3 driven 5mC hydroxylation. In further support of this we observed incorporation of new isotope-labelled deoxycytidine (dC*) in pre-replicating zygotes (Supplementary Fig. 5g,h).

Contrary to previous assumptions, we show that zygotes contain *de novo* DNA methyltransferase activities and both maternally inherited Dnmt1 and Dnmt3a are necessary for the accumulation of paternal 5hmC. Our findings thus support a model whereby Tet3 driven hydroxylation is predominantly implicated in the protection of the newly acquired hypomethylated state from accumulating new DNA methylation. This is achieved through targeting of newly formed 5mC generated by zygotic Dnmt3a and Dnmt1 enzymes or also possibly through preventing Dnmt1 driven methylation maintenance at some regions (Fig. 5b).

Cumulatively, our study explains the previously observed low locus-specific 5hmC levels³⁵, the limited effect of Tet3 knockout on zygotic DNA demethylation^{15, 16} and only limited overlap between 5hmC localisations and regions undergoing DNA demethylation³⁵. We show that epigenetic reprogramming in the early embryo is a complex process underpinned by a dynamic interplay between active DNA demethylation, *de novo* DNA methylation and Tet3-driven 5mC hydroxylation. Finally, although our study provides information regarding the global dynamics of DNA modifications during zygotic reprogramming, further studies

will be necessary to unravel locus specific modification changes and targeting of the key factors involved in this fascinating process.

METHODS

Mice

Outbred MF1 mice and B6CBAF1 used for the *in vitro* fertilisation procedure were purchased from Charles River or Harlan. B6CBAF1 mice were superovulated by intraperitoneal injection of 5U pregnant mare's serum (PMS) and 5U of human chorionic gonadotropin (HCG) 48 hrs later. Dnmt-deficient mice used in this study have been described previously: [Dnmt1^{2lox/2lox}, Zp3-Cre]³², [Dnmt3a^{2lox/2lox}, Zp3-Cre]²² and [Dnmt3L^{-/-}]²⁸. Tet3 conditional knock-out mice has been generated using a 2 steps strategy described in figure 3a. The targeting construct, which generates a null allele, is composed of exon 8 (ENSMUSE00000238680), exon 9 (ENSMUSE00000238677) and a FRT-flanked neomycin cassette, flanked by 2 loxP sites. Following insertion the knock-out allele was rescued in heterozygous Tet3^{-^{WT}} by crossing with a transgenic mice expressing Flp recombinase. Tet3-maternally deleted oocytes (Tet3^{mat-}) were obtained by crossing Gdf9-Cre Tet3^{lox/lox} males with Tet3^{lox/lox} females and by superovulation of 3-weeks old Gdf9-Cre Tet3^{lox/lox} females. All animal experiments were carried out under a UK Home Office Project Licence in a Home-Office designated facility.

In vitro fertilisation of mouse oocytes

The procedure was carried out as in Nagy *et al*⁴⁰. The sperm was isolated from dissected epididymis and capacitated for 1.5 hrs in HTF fertilisation medium (Millipore) supplemented with 4 mg/ml bovine serum albumin (BSA, Sigma-Aldrich). Oocytes were collected 14 hrs post-HCG injection into the same medium.

Tet proteins inhibition was performed by supplementing the fertilisation medium with 1 mM dimethyloxallyl glycine (DMOG, Sigma-Aldrich) or 1 mM deferoxamine (DFX, Sigma-Aldrich) diluted in aqueous buffer; the oocytes were incubated with the drug for at least 40 min before the addition of the sperm. For replication inhibition, 3 ug/ml aphidicolin (Sigma-Aldrich, dissolved in DMSO) was added to the fertilisation medium. As a control, zygotes were incubated with the matching concentration of DMSO (0.1-0.3%). For the quantification of maintenance/*de novo* DNA methylation, oocytes were incubated for at least 40min prior to fertilisation with 7.5 mg/L unlabelled methionine (Fluka) or isotope-labelled (¹³C,₃) methionine (Sigma) and kept in this supplemented medium during IVF. *De novo* DNA methylation was monitored by adding 2 ug/ml aphidicolin to the HTF medium. Incorporation of isotope-labelled dC (dC*) was assessed by incubating oocytes and zygotes with 5mM (¹³C, ¹⁵N) deoxy-cytidine (Silantes) added into the IVF medium.

For culture of preimplantation embryos, zygotes (incubated with DMOG for 8hrs when indicated) were transferred into M16 or KSOM medium (without DMOG) and cultured until morula stage (embryonic day E2.5) or blastocysts stage (E3.5).

Immunofluorescence staining of zygotes

Zygotes collected from natural matings of outbred MF1 mice were cleaned from cumulus cells by 5 min incubation in M2 medium (Sigma-Aldrich) containing 4 mg/ml BSA supplemented with 300 ug/ml hyaluronidase, and fixed for 20 min by 4% paraformaldehyde (PFA) in PBS, followed by three 10 min washes in PBS, 1% BSA. Permeabilisation was performed for 30 min at room temperature in PBS, 1% BSA, 0.5% Triton X-100. Zygotes were then incubated overnight in PBS, 1% BSA, 0.1% Triton X-100 containing the first antibody, washed three times for 10min with PBS, 1% BSA, 0.1% Triton X-100 and incubated for 1hr in the dark with Alexa Fluor 405-, 488- or 568-conjugated IgG secondary antibody (dilution 1:300, Molecular probes) in the same buffer. Zygotes were mounted with ProLong Gold mounting medium containing DAPI (Life Technologies) using imaging spacers and imaged as Z-series confocal (Z step size 0.5 um) sections using a Leica TCS SP5 confocal microscope with a 40x objective.

For Triton pre-extraction, zygotes were incubated in ice-cold permeabilisation solution (50 mM NaCl, 3 mM MgCl₂, 0.5% Triton X-100, 300 mM sucrose in 25 mM HEPES pH 7.4) for 10 min on ice. Zygotes were then washed three times with permeabilisation solution without Triton X-100, fixed for 20 min using 4% PFA in PBS at room temperature and stained as described above. In order to prevent the zona pellucida from collapsing under osmotic stress upon transfer to the mounting media, zygotes were equilibrated in PBS, 1% BSA with increasing concentrations of glycerol before mounting.

5mC and 5hmC staining of mouse zygotes

Staining of DNA modifications has been carried out as described previously¹⁸ with some modifications. Briefly, after 40 min incubation at room temperature in the permeabilisation buffer (PBS, 1% BSA, 0.5% Triton X-100) zygotes were treated with 10 mg/ml RNase A (Roche) in PBS, BSA 1% for 1hr at 37°C. DNA was subsequently denatured using HCl 4 N for 15 min at 37°C. Zygotes were then washed in PBS, 1% BSA for 10 min, incubated in PBS, 1% BSA, 0.1% Triton X-100 for 30 min and incubated in the same buffer with 5mC and 5hmC antibody at 4°C overnight. Zygotes were subsequently washed three times in PBS, 1% BSA, 0.1% Triton X-100 for 10 min and incubated with Alexa Fluor 405-, 488- or 568-conjugated IgG secondary antibodies (dilution 1:300, Molecular Probes) for 1hr at room temperature in the dark. DNA was stained by propidium iodide (PI) (0.25 mg/ml) for 20 min. The final wash was carried out in PBS, 1% BSA for 30 min and the zygotes mounted in ProLong Gold DAPI-free mounting medium (Life Technologies) as described above. Images were analysed using ImageJ software. The mid-section of each pronucleus was identified using PI staining and determined by the maximal area. The mid-section was used to quantify the total intensity of each DNA modification following the subtraction of the signal corresponding to the equal cytoplasmic area (representing staining background). Within each experiment, zygotes have been imaged using the same settings on the microscope (laser power and gain) in order to compare the signal intensity in both pronuclei. When using pat/mat signal ratios, we carefully checked that the maternal intensity remains unchanged between the control and experimental conditions. Statistical analysis was carried out using two-tailed Student's *t*-test with Welsh's correction when required, using GraphPad Prism software.

For 5mC/5hmC dynamics (Fig 1) the staining was additionally carried out using swapped combination of fluorophores and laser channels to control for technical biases. The 5mC/5hmC kinetics was also independently assessed using the same imaging channel for 5mC and 5hmC (using single antibody staining of zygotes). In all cases, the results confirmed our findings presented in Fig. 1C.

Antibodies

XRCC1 (Serotec) 1:200, 5mC (clone 33D3, Diagenode) 1:5000 (0.02 ug/ml), 5hmC (Active Motif) 1:500 (2 ug/ml), H3K9me2 (07-441, Upstate) 1:400, H3K27me3 (gift from Dr. T. Jenuwein) 1:500, H3K4me2 (07-030, Upstate) 1:500, H3K36me3 (gift from Dr. H. Kimura,) 1:50, TET3 (C-term, Abcam) 1:200, Dnmt3a (Imgenex, IMG-268A) 1:200, Dnmt3L (Abnova, PAB2230) 1:100.

Bisulphite sequencing

Polar bodies of zygotes obtained by IVF were removed by micromanipulation and zygotes (10-20 per experiment) were snap frozen in liquid nitrogen. Alternatively, paternal pronuclei were isolated by micromanipulation (10-15 per experiment). Bisulphite sequencing was subsequently carried out using the agarose bead embedding method as described in ⁴¹ or by using the Imprint DNA modification kit (Sigma-Aldrich). The following primers were used for the amplification of Line1 elements: F1: 5'-

GTTAGAGAATTTGATAGTTTTTGGAAATAGG-3'; R1: 5'-

CCAAAACAAAACCTTTCTCAAACACTATAT-3'; F2: 5'-

TAGGAAATTAGTTTGAATAGGTGAGAGGT-3'; R2: 5'-

TCAAACACTATATTACTTTAACAATTCCCA-3'. The semi-nested approach was used: 1st

PCR (F1,R1 primers), 2nd PCR (F1,R2 primers). PCR conditions: 95°C 5min, (95°C 1min,

56°C 1min, 72°C 1min) x35, 72°C 5min. The primers amplify LIMd_Tf and LIMd_Gf

Line1 subtypes. The *p* values were calculated using Mann-Whitney U-test.

Dot blot and competition assay

Plasmid DNA was amplified using a mixture of dATP, dGTP, TTP (Roche) together with either dCTP (Roche), 5-methyl dCTP (Fermentas) or 5-hydroxymethyl dCTP (BioSciences). PCR products were denatured using 0.1N NaOH at 95°C for 5min before cooling on ice. 4-fold serial dilutions were spotted on a nylon membrane (Hybond-N⁺, GE Healthcare); the membrane was UV-crosslinked (254 nm, 1200J/m²), blocked in TBS, 0.1% Tween-20, 5% milk and incubated with primary antibodies overnight at 4°C in TBS, 0.1% Tween-20, 1% milk. After three washes, the membrane was incubated with HRP-conjugated IgG secondary antibodies for 1 hr at room temperature in the same buffer. Chemiluminescence detection was carried out using ECL Western Blotting Reagents (GE Healthcare). Spotted DNA was detected by staining the membrane in 0.02% methylene blue.

For the competition assay, NIH3T3 cells were transfected with a pCAG-IRES-GFP plasmid containing the full-length *Tet1* (NM_001253857) or *Tet3* (NM_183138) cDNA, respectively. DNA was extracted using QIAamp DNA Blood Mini Kit (Qiagen) and processed for dot blot as described above. Anti-5hmC antibody (0.2 ug/ml) was pre-incubated in TBS, 0.1% Tween-20, 1% milk for 2 hrs at 4°C with 50 mM (corresponding to a 200-fold excess) of

nucleosides: deoxycytidine (Sigma-Aldrich), 5-methyl-2'-deoxycytidine (RI Chemicals) or 5-hydroxymethyl-2'-deoxycytidine (Berry & Associates). The membranes were incubated with the staining mix overnight at 4°C and processed as described above.

TET1 *in vitro* enzymatic assay

0.5 ug of recombinant TET1 protein (Actif Motif, #31363) was incubated with 100 ng of 5mC-enriched PCR product according to manufacturer instruction for 3 hrs at 37°C in the presence of DMOG (10 or 25 mM) or DFX (10 or 20 mM). Reaction was then spotted on a nylon membrane and processed for dot blot.

Somatic Cell Nuclear Transfer

The parental ES cell line E14Tg2a.4 (referred as WT-ESC) has been obtained from BayGenomics (MMRRC #015890-UCD-ULTRA). DNA methyltransferase triple knock out embryonic stem cell (Dnmt1^{-/-}, Dnmt3a^{-/-}, Dnmt3b^{-/-} DNMT-TKO, clone 19, obtained from RIKEN Bio Resource Center #RBRC-AES0146 and described in³³) were cultured in GMEM (Gibco), 15% FBS (Sigma), 0.1 mM non-essential amino-acids (Gibco), 1 mM sodium pyruvate (Sigma), 2000 U/ml ESGRO mouse LIF (Millipore), 0.1 mM 2-mercaptoethanol (Gibco) without feeders. Prior to electrofusion, cells were arrested at metaphase by incubation with 0.5 ug/ml nocodazole (Sigma-Aldrich) for 4 hrs. MII-oocytes were incubated in HEPES-buffered CZB medium supplemented with 5 µg/ml cytochalasin B (Sigma-Aldrich) for 10 min at room temperature. Enucleation was performed as reported^{42, 43}. Briefly, after 10 min treatment, MII-oocytes were transferred into 10 µl of the same medium covered with mineral oil (Sigma-Aldrich) on the lid of a culture dish. All micromanipulations were performed under an inverted microscope equipped with Hoffman optics using a piezo driven system (Prime Tech Ltd., Ibaraki, Japan). After removal of metaphase chromosomes, a wild type or DNMT-TKO ES cell arrested at metaphase was introduced into the perivitelline space of the enucleated oocyte⁴⁴. The fusion of donor and recipient was induced by a DC pulse of 2500 V/cm for 10 µs using an ECM 830 (BTX, San Diego, CA) in 300 mM mannitol, 0.1mM MgSO₄, 0.1 mg/ml polyvinyl alcohol and 3 mg/ml bovine serum albumin. The fusion rates were determined 1 hr after the pulse by microscopic examination. Fused pairs were activated by treatment with 10 mM SrCl₂ in calcium-free CZB medium for 1 hr. The reconstructed embryos were cultured in M16 medium (Millipore) in 5 % CO₂ in air at 37°C.

Reverse transcription and quantitative PCR analysis

Total RNA was purified using Trizol (Life Technologies) following manufacturer's instructions. Random-primed reverse transcription was performed using PrimeScript RT Reagent Kit with gDNA Eraser (Perfect Real Time, Takara Bio). cDNA corresponding to 1.5 to 3 zygotes in 3 ul was added to 10 ul of quantitative PCR mix containing SensiMix SYBR No-ROX (Bioline). Real-time quantitative PCR reactions were performed on a CFX96 real-time PCR detection system (Bio-Rad). The standard curve method using ES cells cDNA was used for quantification. Primers: *H3f3a_F5'*-CCATGCCAAACGTGTAACAA-3'; *H3f3a_R* 5'-TACCTTTGACCCCATGGAAA-3'; *Tet3 exon 3_F5'*-GCCTCCTCCCTACTTCCAC-3'; *Tet3 exon 3_R 5'*-CCTGGACCTGGATTCTTGA-3'; *Tet3 exon11_F5'*-TTGACTGGTCCCAGCCTAAC-3'; *Tet3 exon11_R 5'*-

TGAAGGGATCCCACAGTTTC-3'. Two-tailed unpaired *t*-test was performed by using GraphPad Prism software.

Parthenogenetic activation of oocytes

MII oocytes were incubated with KSOM medium where Ca²⁺ has been replaced with 10 mM strontium (Sigma) supplemented with 5 ug/ml cytochalasin B (Sigma) for 1.5hrs. Parthenogenetically activated oocytes were then transferred into HTF medium supplemented with 2 ug/ml aphidicolin and 5 ug/ml cytochalasin B. Completion of S-phase was monitored by incubating the parthenotes for 45 min in HTF medium supplemented with 400 uM EdU before staining as described below.

EdU staining in zygotes using Click-IT chemistry

To verify replication inhibition by aphidicolin and the completion of S-phase in parthenogenetically activated oocytes, embryos were incubated with 400 uM of 5-ethynyl deoxyuridine (EdU, Life Technologies) during development prior to removal of zona pellucida and fixation for 20 min in PFA 4% at room temperature. When indicated, pulse of EdU was performed by incubation the zygotes for 30min prior to zona pellucida removal and fixation.

EdU staining followed manufacturer's instruction (Click-iT Nascent RNA capture kit, Life Technologies). Briefly, zygotes were permeabilised in PBS, 1% BSA, 0.5% Triton X-100 for 30min at room temperature, washed twice in PBS, 1% BSA and incubated for 1 hr in dark with a Click-IT reaction mix containing 2.5 ul of Alexa Fluor Azide 488. Zygotes were subsequently washed several times in PBS, 1% BSA and mounted in Prolong DAPI Mounting medium.

DNA isolation from sperm, oocytes and early stage embryos

Sperm DNA from B6CBAF1 was isolated using a protocol modified from ⁴⁵. Fresh sperm from dissected epididymis was left to settle in HTF medium. Supernatant containing active sperm was centrifuged for 2 min at 1100g and resuspended in 200 ul of solution A (75 mM NaCl and 25 mM EDTA) and 200 ul of solution B (10 mM Tris-HCl pH 8, 10 mM EDTA, 2% SDS, 80 mM DTT) complemented with 1 ug of RNase A (Qiagen) and incubated for 1 hr at 37°C. 100 ug of Proteinase K (Roche) per 0.5 ml of solution A+B was subsequently added and incubated overnight at 55°C. Sperm genomic DNA was further purified using phenol:chloroform:isoamyl alcohol extraction followed by ethanol precipitation; DNA pellet was resuspended in LC/MS quality grade water (Fisher Scientific).

Genomic DNA from oocytes and 2 cell embryos was isolated using DNA Micro Kit (Qiagen) according to manufacturer's instruction, without RNA carrier. DNA was eluted in LC/MS quality grade water (Fisher Scientific). For samples of zygotes (when indicated), both polar bodies were first carefully removed by micromanipulation (Narishige Co., Tokyo, Japan) before DNA extraction.

Liquid chromatography-mass spectrometry

Genomic DNA of 600-200 cells was used for quantification of DNA modifications. DNA was digested to nucleosides using 1 U of benzonase (Novagen), 0.5 mM phosphodiesterase I (SIGMA) and 200 mU of alkaline phosphatase in 20 mM Tris-HCl pH 7.9, 4 mM MgCl₂ for a minimum of 6 hours at 37°C, or using a digestion enzymatic mix (NEB). Samples were pre-cleaned by acetonitrile precipitation. All samples and standard curve points were spiked with isotope-labelled synthetic nucleosides (100 fmol of dC* and dG*, 5 fmol of 5mC*, 500 amol of 5hmC*) obtained from T. Carell (Center for Integrated Protein Science at the Department of Chemistry, Ludwig-Maximilians-Universität München, München, Germany). The nucleosides were separated on an Agilent RRHD Eclipse Plus C18 2.1 × 100 mm 1.8u column by using the UHPLC 1290 system (Agilent) and analysed using Agilent 6490 triple quadrupole mass spectrometer. To calculate the concentrations of individual nucleosides, standard curves representing the ratio of the peak response of known amounts of synthetic nucleosides spiked with the same matrix as the samples and the peak response of the isotope-labelled nucleosides were generated and used to convert the peak-area values to corresponding concentrations. Threshold for quantification are: signal-to-noise (calculated with a peak-to-peak method) above 10 and the limit of quantification as detailed for each nucleosides in the Supplementary Fig. 4a. For non-quantifiable peaks (n.d.), an overestimation of 5mC/dG or 5hmC/dG ratio is calculated based on the limit of detection for both nucleosides.

Reproducibility of experiments

NCB policy precludes the use of statistical analysis for data where $n < 3$ biological replicates. However in our LC/MS experiments, we observed a very low variation between biological replicates with a coefficient of variation below 10 for 5mC (Fig. 2b,c, 3e,f, and Supplementary Fig. 4c,e,h). Additionally, LC/MS results are technically supported by immunofluorescence data (Fig. 2a, 3d and Supplementary Fig. 2b, 4i) and bisulphite sequencing analysis (Supplementary Fig. 3d-f, 4j), and conceptually by alternative approaches (conditional knockout mouse model and small molecule inhibitors of dioxygenases). It should also be noted that each LC/MS measurement reflects DNA modifications quantification of a pool of about 100 embryos, analysed in technical duplicates. LC/MS data (Figure 2b, DNA modifications in zygotes without polar bodies) represent 3 biological replicates (except for the DMOG-treated data point); replicate of this experiment (zygotes with polar bodies) is shown in Supplementary Figure 4e. LC/MS results presented in Figure 2c, 4a and Supplementary Figures 4c, 4e, 4h and 5g are based on 2 biological replicates (each carried out in technical duplicates).

Immunofluorescence data presented in Figure 2a and Supplementary Figure 2b have been reproduced 4 times independently, Figure 3d, 4c, 4d and Supplementary Figures 2f, 3c, 5b twice independently. It should be noted that for the quantification of DNA modifications in zygotes by immunofluorescence, each embryo represents a biological replicate.

Statistics derived from bisulphite sequencing analysis (Supplementary Fig. 3d-f, 4j) rely on the number of clones amplified; experiments presented in Supplementary Figure 3d,e have been reproduced twice independently.

Supplementary Material

Refer to Web version on PubMed Central for supplementary material.

ACKNOWLEDGEMENTS

We are grateful to the members of Hajkova lab (especially Kirsten McEwen) and to Naveenan Navaratnam for discussions and revision of the manuscript. We thank T. Carell for providing the isotope-labelled synthetic nucleosides. We would like to acknowledge the MRC CSC Microscopy facility for help with imaging of the embryos, and Megan Woodberry, Darran Hardy and Justyna Glegola for mouse husbandry. We would like to thank MRC transgenic facility for their help regarding IVF. The LC/MS analysis was conducted in collaboration with Agilent Technologies, whom we would like to thank for generous support and help. This work was supported by MRC (MC_US_A652_5PY70) and EpigeneSys network funding to P.H. R.A. was a recipient of the Marie Curie Intra-European Fellowship (FP7). B.N was a recipient of the Marie Curie Incoming-European Fellowship (FP7).

REFERENCES

1. Wossidlo M, et al. 5-Hydroxymethylcytosine in the mammalian zygote is linked with epigenetic reprogramming. *Nat Commun.* 2011; 2:241. [PubMed: 21407207]
2. Zhang P, et al. The involvement of 5-hydroxymethylcytosine in active DNA demethylation in mice. *Biol Reprod.* 2012; 86:104. [PubMed: 22262693]
3. Gu TP, et al. The role of Tet3 DNA dioxygenase in epigenetic reprogramming by oocytes. *Nature.* 2011; 477:606–610. [PubMed: 21892189]
4. Iqbal K, Jin SG, Pfeifer GP, Szabo PE. Reprogramming of the paternal genome upon fertilization involves genome-wide oxidation of 5-methylcytosine. *Proc Natl Acad Sci U S A.* 2011; 108:3642–3647. [PubMed: 21321204]
5. Oswald J, et al. Active demethylation of the paternal genome in the mouse zygote. *Curr Biol.* 2000; 10:475–478. [PubMed: 10801417]
6. Mayer W, Niveleau A, Walter J, Fundele R, Haaf T. Demethylation of the zygotic paternal genome. *Nature.* 2000; 403:501–502. [PubMed: 10676950]
7. Santos F, et al. Active demethylation in mouse zygotes involves cytosine deamination and base excision repair. *Epigenetics & chromatin.* 2013; 6:39. [PubMed: 24279473]
8. Ito S, et al. Tet proteins can convert 5-methylcytosine to 5-formylcytosine and 5-carboxylcytosine. *Science.* 2011; 333:1300–1303. [PubMed: 21778364]
9. He YF, et al. Tet-mediated formation of 5-carboxylcytosine and its excision by TDG in mammalian DNA. *Science.* 2011; 333:1303–1307. [PubMed: 21817016]
10. Inoue A, Shen L, Dai Q, He C, Zhang Y. Generation and replication-dependent dilution of 5fC and 5caC during mouse preimplantation development. *Cell Res.* 2011; 21:1670–1676. [PubMed: 22124233]
11. Tahiliani M, et al. Conversion of 5-methylcytosine to 5-hydroxymethylcytosine in mammalian DNA by MLL partner TET1. *Science.* 2009; 324:930–935. [PubMed: 19372391]
12. Wossidlo M, et al. Dynamic link of DNA demethylation, DNA strand breaks and repair in mouse zygotes. *EMBO J.* 2010; 29:1877–1888. [PubMed: 20442707]
13. Smith ZD, et al. A unique regulatory phase of DNA methylation in the early mammalian embryo. *Nature.* 2012; 484:339–344. [PubMed: 22456710]
14. Huang Y, et al. The behaviour of 5-hydroxymethylcytosine in bisulfite sequencing. *PLoS One.* 2010; 5:e8888. [PubMed: 20126651]
15. Shen L, et al. Tet3 and DNA replication mediate demethylation of both the maternal and paternal genomes in mouse zygotes. *Cell stem cell.* 2014; 15:459–470. [PubMed: 25280220]
16. Guo F, et al. Active and passive demethylation of male and female pronuclear DNA in the Mammalian zygote. *Cell stem cell.* 2014; 15:447–458. [PubMed: 25220291]
17. Santos F, Hendrich B, Reik W, Dean W. Dynamic reprogramming of DNA methylation in the early mouse embryo. *Dev Biol.* 2002; 241:172–182. [PubMed: 11784103]

18. Hajkova P, et al. Genome-wide reprogramming in the mouse germ line entails the base excision repair pathway. *Science*. 329:78–82. [PubMed: 20595612]
19. Rougier N, et al. Chromosome methylation patterns during mammalian preimplantation development. *Genes Dev*. 1998; 12:2108–2113. [PubMed: 9679055]
20. Shirane K, et al. Mouse oocyte methylomes at base resolution reveal genome-wide accumulation of non-CpG methylation and role of DNA methyltransferases. *PLoS Genet*. 2013; 9:e1003439. [PubMed: 23637617]
21. Smallwood SA, et al. Dynamic CpG island methylation landscape in oocytes and preimplantation embryos. *Nat Genet*. 2011; 43:811–814. [PubMed: 21706000]
22. Kaneda M, et al. Essential role for de novo DNA methyltransferase Dnmt3a in paternal and maternal imprinting. *Nature*. 2004; 429:900–903. [PubMed: 15215868]
23. Tomizawa S, et al. Dynamic stage-specific changes in imprinted differentially methylated regions during early mammalian development and prevalence of non-CpG methylation in oocytes. *Development*. 2011; 138:811–820. [PubMed: 21247965]
24. Bourc'his D, Xu GL, Lin CS, Bollman B, Bestor TH. Dnmt3L and the establishment of maternal genomic imprints. *Science*. 2001; 294:2536–2539. [PubMed: 11719692]
25. Guenatri M, Duffie R, Iranzo J, Fauque P, Bourc'his D. Plasticity in Dnmt3L-dependent and -independent modes of de novo methylation in the developing mouse embryo. *Development*. 2013; 140:562–572. [PubMed: 23293288]
26. Hirasawa R, et al. Maternal and zygotic Dnmt1 are necessary and sufficient for the maintenance of DNA methylation imprints during preimplantation development. *Genes Dev*. 2008; 22:1607–1616. [PubMed: 18559477]
27. Kaneda M, et al. Genetic evidence for Dnmt3a-dependent imprinting during oocyte growth obtained by conditional knockout with Zp3-Cre and complete exclusion of Dnmt3b by chimera formation. *Genes Cells*. 2010
28. Hata K, Okano M, Lei H, Li E. Dnmt3L cooperates with the Dnmt3 family of de novo DNA methyltransferases to establish maternal imprints in mice. *Development*. 2002; 129:1983–1993. [PubMed: 11934864]
29. Kurihara Y, et al. Maintenance of genomic methylation patterns during preimplantation development requires the somatic form of DNA methyltransferase 1. *Dev Biol*. 2008; 313:335–346. [PubMed: 18048024]
30. Cirio MC, et al. Preimplantation expression of the somatic form of Dnmt1 suggests a role in the inheritance of genomic imprints. *BMC Dev Biol*. 2008; 8:9. [PubMed: 18221528]
31. Pfeiffer MJ, et al. Proteomic analysis of mouse oocytes reveals 28 candidate factors of the “reprogrammome”. *J Proteome Res*. 2011; 10:2140–2153. [PubMed: 21344949]
32. Jackson-Grusby L, et al. Loss of genomic methylation causes p53-dependent apoptosis and epigenetic deregulation. *Nat Genet*. 2001; 27:31–39. [PubMed: 11137995]
33. Tsumura A, et al. Maintenance of self-renewal ability of mouse embryonic stem cells in the absence of DNA methyltransferases Dnmt1, Dnmt3a and Dnmt3b. *Genes Cells*. 2006; 11:805–814. [PubMed: 16824199]
34. Salvaing J, et al. 5-Methylcytosine and 5-hydroxymethylcytosine spatiotemporal profiles in the mouse zygote. *PLoS One*. 2012; 7:e38156. [PubMed: 22693592]
35. Wang L, Zhang J, Duan J, Gao X, Zhu W, Lu X, Yang L, Zhang J, Li G, Ci W, Li W, Zhou Q, Aluru N, Tang F, He C, Huang X, Liu J. Programming and Inheritance of Parental DNA Methylomes in Mammals. *Cell*. 2014; 157:979–991. [PubMed: 24813617]
36. Inoue A, Zhang Y. Replication-dependent loss of 5-hydroxymethylcytosine in mouse preimplantation embryos. *Science*. 2011; 334:194. [PubMed: 21940858]
37. Peat JR, et al. Genome-wide Bisulfite Sequencing in Zygotes Identifies Demethylation Targets and Maps the Contribution of TET3 Oxidation. *Cell reports*. 2014; 9:1990–2000. [PubMed: 25497087]
38. Adenot PG, Mercier Y, Renard JP, Thompson EM. Differential H4 acetylation of paternal and maternal chromatin precedes DNA replication and differential transcriptional activity in pronuclei of 1-cell mouse embryos. *Development*. 1997; 124:4615–4625. [PubMed: 9409678]
39. Tang F, et al. RNA-Seq analysis to capture the transcriptome landscape of a single cell. *Nat Protoc*. 2010; 5:516–535. [PubMed: 20203668]

40. Nagy, A., editor. *Manipulating the mouse embryo: a laboratory manual*. Edn. 3rd. 2003.
41. Hajkova P, et al. DNA-methylation analysis by the bisulfite-assisted genomic sequencing method. *Methods Mol Biol*. 2002; 200:143–154. [PubMed: 11951649]
42. Ogura A, Inoue K, Takano K, Wakayama T, Yanagimachi R. Birth of mice after nuclear transfer by electrofusion using tail tip cells. *Mol Reprod Dev*. 2000; 57:55–59. [PubMed: 10954856]
43. Kishigami S, et al. Production of cloned mice by somatic cell nuclear transfer. *Nat Protoc*. 2006; 1:125–138. [PubMed: 17406224]
44. Ono Y, et al. Production of cloned mice from embryonic stem cells arrested at metaphase. *Reproduction*. 2001; 122:731–736. [PubMed: 11690533]
45. Walsh CP, Bestor TH. Cytosine methylation and mammalian development. *Genes Dev*. 1999; 13:26–34. [PubMed: 9887097]

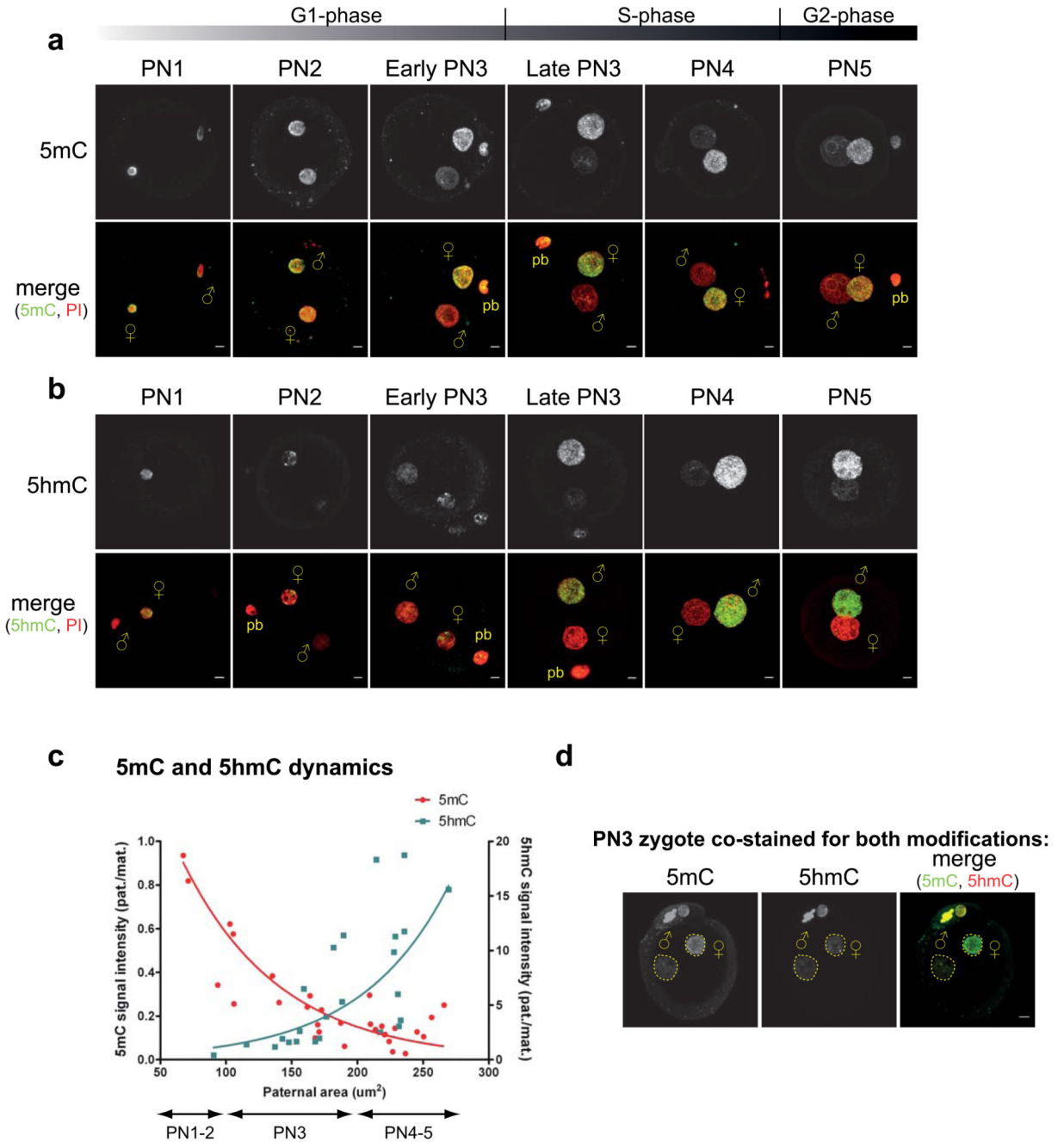


Figure 1. 5hmC and 5mC kinetics during mouse zygotic development. 5mC (a) and 5hmC (b) enrichment in mouse zygotes at different developmental stages as in ³⁸ assessed by immunofluorescence using 5mC and 5hmC specific antibodies. DNA is stained using PI. Representative images are shown and correspond to the 5mC and 5hmC signals quantification presented in (c). (c) Quantification of 5mC (red line, left axis) and 5hmC (green line, right axis) staining is shown as a ratio between signal from paternal pronucleus relative to the signal from maternal pronucleus. Values are plotted against the area of the

mid-sections of the paternal pronuclei. Each data point represents a zygote. Experiment reproduced 3 times (n>100) **(d)** Loss of paternal 5mC and accumulation of 5hmC are temporally separated. Early PN3 zygotes do not show any detectable 5mC or 5hmC in paternal pronucleus. 5mC, 5-methylcytosine; 5hmC, 5-hydroxymethylcytosine; PN, pronuclei; PI, propidium iodide; ♀, female pronucleus; ♂, male pronucleus; pb, polar body. (Scale bars, 5µm.)

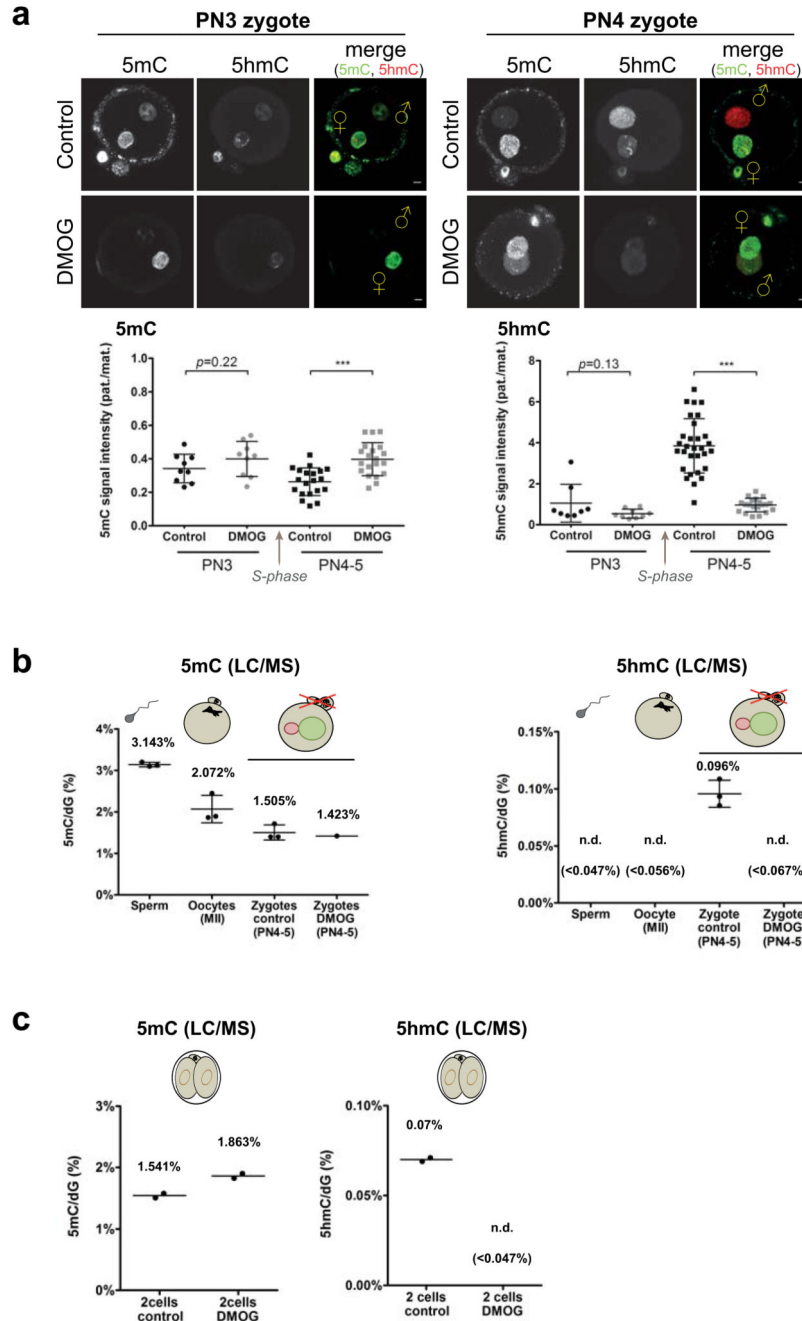
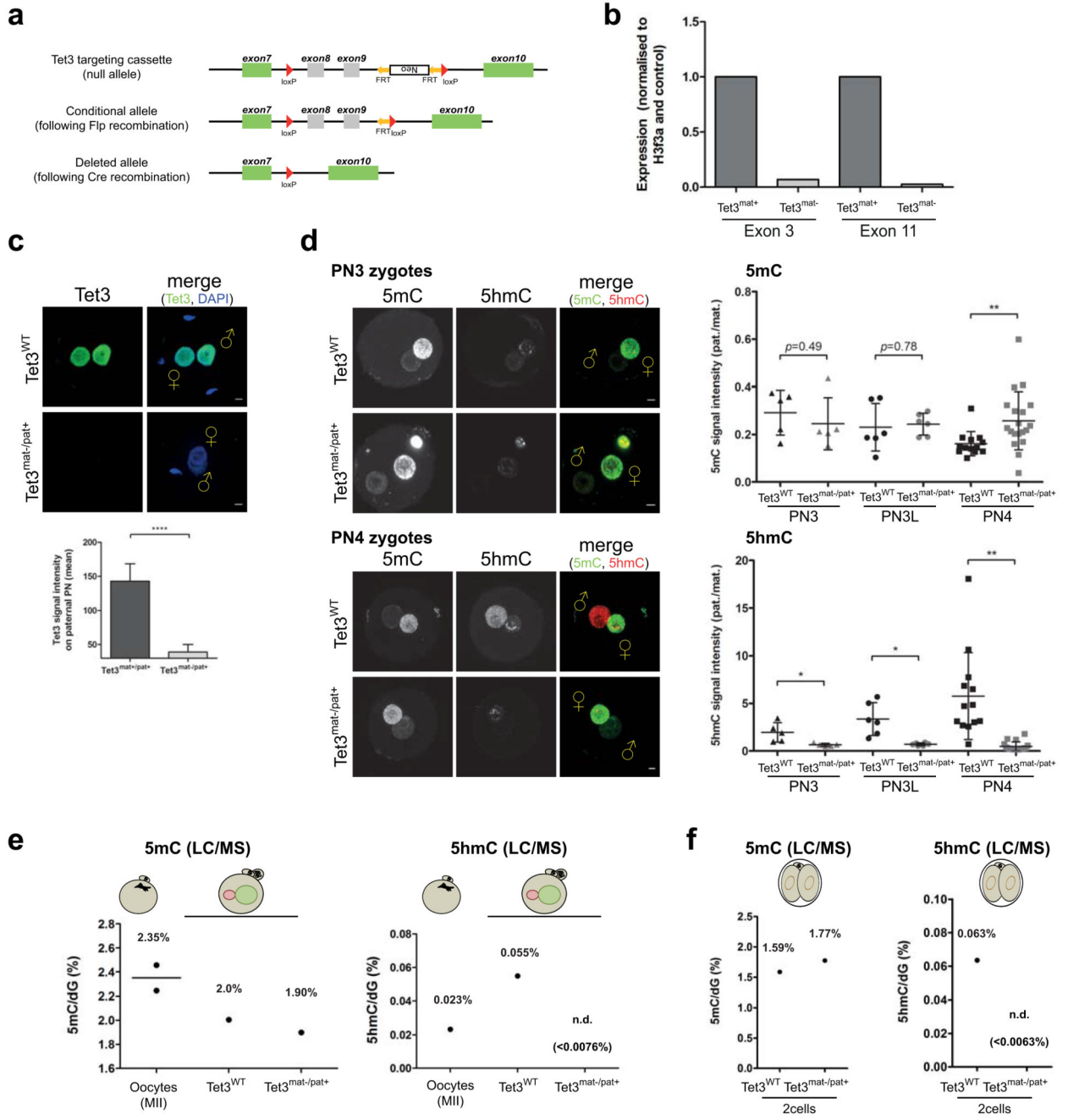


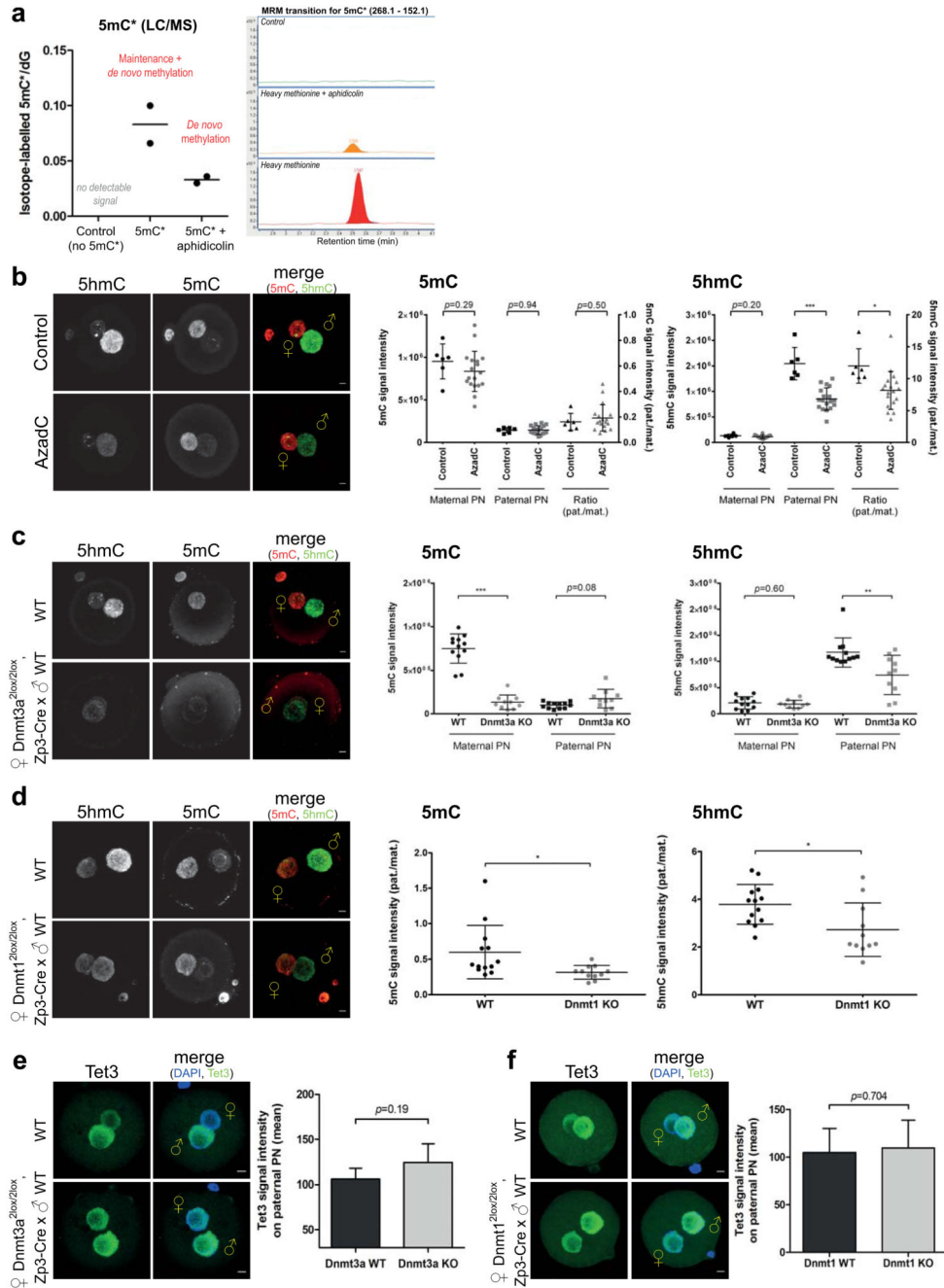
Figure 2. Small molecule inhibition of Tet protein activity abrogates 5hmC formation but does not prevent DNA demethylation. **(a)** 5mC and 5hmC staining of control and DMOG-treated zygotes (IVF). Quantification of both DNA modifications is represented as a ratio between the pronuclear signals (pat/mat). For 5mC staining, n=18 PN3 zygotes and n=40 PN4-5 zygotes; for 5hmC staining, n=17 PN3 zygotes and n=48 PN4-5 zygotes. This experiment has been replicated 4 times independently. **(b)** Quantification of 5mC/dG and 5hmC/dG ratio in sperm, MII oocytes, and in zygotes without polar bodies (control or treated with DMOG)

by LC/MS (n=3 independent experiments with 2 technical replicates each, except for DMOG-treated zygotes; replicate of this experiment in Supplementary Fig. 4e). Limits of quantification are summarised in Supplementary Fig. 4a. For peaks below quantification limit, an overestimation of 5hmC/dG ratio is calculated based on the limit of detection of 5hmC. (c) Quantification of DNA modifications in 2-cell embryos derived from DMOG-treated or control zygotes analysed by LC/MS (n=2 independent experiments and 2 technical replicates for each point). Statistical analysis was carried out using Student's *t*-test (two-sided). Error bars indicate s.d. DMOG, dimethylallyl glycine; ♀, female pronucleus; ♂, male pronucleus. n.d., non-detectable; ***, $p < 0.001$. (Scale bars, 5µm.)

**Figure 3.**

Tet3 is not required for loss of 5mC in early zygote. **(a)** Scheme of the targeting strategy used to generate Tet3 conditional mice. **(b)** RT-qPCR analysis of *Tet3* mRNA (exon3 and exon11) in control (Tet3^{mat+}) and Tet3-depleted oocytes (Tet3^{mat-}). Results are normalised to endogenous *H3f3a* and to control (Tet3^{mat+}). Bars represent the mean of 3 technical replicates. **(c)** Tet3^{WT} (n=10) and Tet3^{mat-/pat+} (n=8) zygotes were stained for Tet3 protein. Quantification is represented as the mean of intensity on the paternal pronuclei after background subtraction. **(d)** Tet3^{WT} and Tet3^{mat-/pat+} zygotes were co-stained for 5mC and

5hmC at different time points post-fertilisation. Quantification of both DNA modifications is presented as a ratio of paternal over maternal signal intensity. Each data point represents an independent zygote (n=5 PN3, n=6 PN3L and n=13 Tet3^{WT} zygotes; n=5 PN3, n=6 PN3L and n=19 Tet3^{mat-/pat+} zygotes; 2 independent experiments). (e) Quantification of 5mC/dG and 5hmC/dG in Tet3^{WT} and Tet3^{mat-/pat+} zygotes (with polar bodies) by LC/MS. Each point represents the mean of 2 technical replicates of a pool of about 100 oocytes or embryos. (f) Quantification of DNA modifications in 2-cell embryos derived from Tet3^{WT} or Tet3^{mat-/pat+} zygotes analysed by LC/MS. Each point represents the mean of 2 technical replicates of a pool of about 50 embryos. Statistical analysis was carried out using Student's *t*-test (two-sided). Error bars indicate s.d. PN3L, late PN3; ♀, female pronucleus; ♂, male pronucleus. n.d., non-detectable; *, *p*<0.05; **, *p*<0.01; ****, *p*<0.0001 (Scale bars, 5um.)

**Figure 4.**

Hydroxylation targets newly deposited 5mC generated by Dnmt3a and Dnmt1. (a) Isotope-labelled 5mC (5mC*) quantified by LC/MS after incubation of zygotes with heavy methionine ($^{13}C, d_3$ -methyl) in the presence or absence of aphidicolin (IVF). Each point represents a biological replicate (n=2). An example of the 5mC* peak detected by LC/MS is depicted for each condition and further confirms the existence of both maintenance and *de novo* DNA methylation in zygotes. Note that the observed signal represents only a fraction of new zygotic 5mC due to the endogenous pool of unlabelled S-adenosyl-methionine. (b)

Inhibition of new zygotic DNA methylation by 5-azadeoxycytidine (azadC) (IVF) affects accumulation of paternal 5mC as assessed by staining using 5mC and 5hmC specific antibodies. Only zygotes with a paternal mid-section area $> 200\mu\text{m}^2$ (~PN4-5 zygotes) were considered to avoid developmental staging bias. Quantification of 5mC and 5hmC is represented as signal intensity in paternal and maternal pronuclei (left axis) or as a ratio between the pronuclei signal (pat/mat) (right axis). (n=6 control and n=18 treated zygotes; experiment replicated twice independently). 5mC and 5hmC staining in PN4-5 zygotes (paternal mid-section area $>200\mu\text{m}^2$) with maternal (c) Dnmt3a ($[\text{♀}Dnmt3a^{2lox/2lox}, Zp3-Cre] \times \text{♂}WT$) (n=12 WT and n=10 KO zygotes; experiment reproduced twice independently) or (d) Dnmt1 ($[\text{♀}Dnmt1^{2lox/2lox}, Zp3-Cre] \times \text{♂}WT$) (n=13 WT and n=11 KO zygotes; experiments reproduced twice independently) deletion. Note that only total signal intensity is plotted in (c) as Dnmt3a deletion affects 5mC and 5hmC level in maternal PN. (e, f) Tet3 localisation and signal intensity is identical between (e) WT (n=4) and Dnmt3a KO (n=3) or (f) WT (n=5) and Dnmt1 KO (n=3) zygotes. Quantification is represented as the mean of intensity on the paternal pronuclei after background subtraction. Statistical analysis was carried out using Student's *t*-test (two-sided). Error bars indicate s.d. *, $p<0.05$; **, $p<0.01$; ***, $p<0.001$. ♀, female pronucleus; ♂, male pronucleus; azadC, 5-azadeoxycytidine. (Scale bars, 5 μm .)

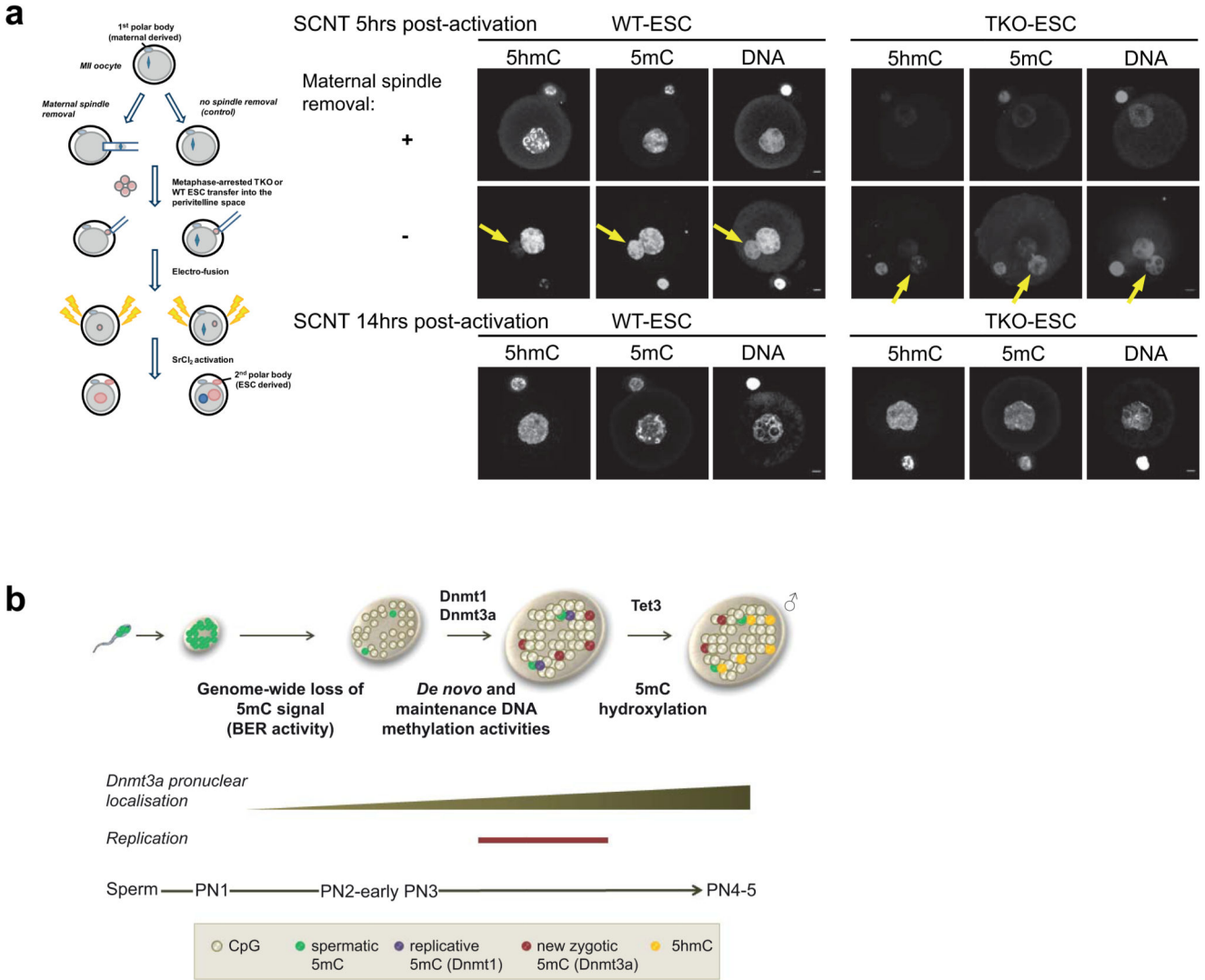


Figure 5. *De novo* DNA methylation activity is present in the oocyte and generates a target for hydroxylation in SCNT experiment. **(a)** Schematic of the somatic cell nuclear transfer (SCNT) experiment using wild-type (WT) or triple Dnmt knockout [*Dnmt1*^{-/-} *Dnmt3a*^{-/-} *Dnmt3b*^{-/-}] (TKO) ES cells. 5mC and 5hmC staining following SCNT into enucleated oocyte using WT (left panel) or a TKO (right panel) ES cells. Staining was carried out 5 and 14 hours post-activation of the reconstituted embryos. As a control, staining of maternal genome (indicated by an arrow) in embryos following SCNT into non-enucleated oocyte (lower panel). The increase of 5mC and 5hmC intensity on the TKO nuclei 14hrs post-activation reflects *de novo* DNA methylation activity in the oocyte, targeted by Tet3-hydroxylation. Representative images are shown (n=7 and n=6 WT-ESC and TKO pseudopronuclei respectively) (Scale bars, 5µm.) **(b)** Following genome-wide loss of spermatc 5mC in the male pronucleus of mouse zygote, newly deposited 5mC produced by zygotic Dnmt1 and Dnmt3a is hydroxylated by Tet3 (model).